

# Particles on curved surfaces - a dynamic approach by a phase field crystal model

Rainer Backofen,<sup>\*</sup> Axel Voigt,<sup>†</sup> and Thomas Witkowski<sup>‡</sup>

*Department of Mathematics, Technische Universität Dresden, 01062 Dresden, Germany*

(Dated: May 7, 2019)

We present a dynamic model to study ordering of particles on arbitrary curved surfaces. Thereby the particles are represented as maxima in a density field and a surface partial differential equation for the density field is solved to the minimal energy configuration. We study annihilation of dislocations within the ordered system and premelting along grain-boundary scars. The obtained minimal energy configurations on a sphere are compared with existing results and scaling laws are computed for the number of excess dislocations as a function of system size.

PACS numbers:

Problems related to optimal ordering of particles on curved surfaces date back to the classical Thomson problem [1] to find the ground state of  $N$  particles on a sphere interacting with a Coulomb potential. A classic theorem of Euler shows for a triangulation of the surface in which nearest neighbors are connected, that  $\sum_i (6 - i)v_i = 6\chi$ , with  $v_i$  as the number of vertices with  $i$  nearest neighbors and  $\chi$  as the Euler characteristic of the surface. Thus for surfaces with the topology of a sphere ( $\chi = 2$ ), besides the expected triangular lattice with six-fold coordination, which would give the optimal packing in a plane, there must be at least 12 five-fold disclinations present. With each disclination an extra energy is associated (relative to a perfect triangular lattice in flat space) which grows proportional to  $r^2$ , with  $r$  as the radius of the sphere. For a fixed lattice constant  $a$  we have  $N \sim (r/a)^2$ . Thus for large  $N$  mechanisms are expected which reduce this extra energy by changing the ground-state configuration. One mechanism is a buckling transition of the disclinations, which form sharp corners and turn the sphere into a polygon. The transition depends on Young's modulus  $Y$  and bending rigidity  $b$  via the Foppl-von Karman number  $Yr^2/b$  and is intensively studied for viral capsids where protein subunits play the role of the particles [2, 3]. In cases where large surface tension limits significant buckling the energy can be reduced by introducing grain-boundary scars. Realizations are for example water droplets in oil, which are coated with colloidal particles [4]. Such coated droplets are potential drug delivery vehicles [5, 6]. Similar configurations occur if a jammed layer of colloidal particles separates two immiscible fluids forming a so-called bijel [7], which has potential applications as an efficient micro-reacting media. A large number of ordered particles on curved surfaces is also required for fabrication of nanostructures on pliable substrates, e.g. to make foldable electronic devices [8]. For all these applications a detailed understanding of the grain boundary scars is of interest as they may be sources of leaks,

influence mechanical properties or lead to failure in electronic devices. We introduce an efficient way to compute the dynamics of these grain boundary scars and dislocations associated with them and provide an approach to compute optimal ordering of many particles on arbitrarily curved surfaces. As the grain boundary scars belong to the thermal and mechanical equilibrium our approach is based on energy minimization with the geometric frustration resulting from the curved surface incorporated.

For  $2 \leq N \leq 100$  there is agreement of all numerical and theoretical methods for the Thomson problem, suggesting that the global minimum configuration has been found. However, for large  $N$ , owing to an exponential growth in local minima [9], finding global minima becomes extremely difficult. Grain boundary scars are expected for  $N > 360$ . Numerical approaches to solve such problems are typically based on genetic algorithms, steepest decent minimization or coarse grained approaches, in which the elasticity field between grain boundary scars is solved [10, 11]. All approaches are devoted to finding the ground state. Dynamic models have been considered [12] which allow us to describe experimentally observed dislocation glide within the grain boundary scars [13, 14]. We will introduce an approach without any coarse graining by directly addressing the dynamic evolution and rearrangement of the particles on an arbitrary curved surface. Our approach is based on a free energy functional for a number density. In the plane such free energy functionals have been used to characterize patterns. The simplest possible form of a free energy which produces periodic structures in a domain  $\Omega$  reads

$$\mathcal{F}[\rho] = \int_{\Omega} -|\nabla\rho|^2 + \frac{1}{2}|\Delta\rho|^2 + f(\rho) d\Omega \quad (1)$$

with  $\rho$  as the number density and  $f(\rho) = \frac{1}{2}(1-\epsilon)\rho^2 + \frac{1}{4}\rho^4$  as a potential with a parameter  $\epsilon$ . The equilibrium state for  $\Omega = \mathbb{R}^2$  has a perfect six-fold symmetry. Evolutional laws associated with this energy are the  $L^2$ -gradient flow  $\partial_t\rho = -\delta\mathcal{F}/\delta\rho$ , the Swift-Hohenberg model [15], and the  $H^{-1}$  gradient flow  $\partial_t\rho = \Delta\delta\mathcal{F}/\delta\rho$ , the phase field crystal (PFC) model [16]. The evolutions naturally contain elastic energy, as an expansion of the free energy around the equilibrium period spacing results in the potential energy of a spring, i.e. Hooke's law. As the energy

<sup>\*</sup>Electronic address: rainer.backofen@tu-dresden.de

<sup>†</sup>Electronic address: axel.voigt@tu-dresden.de

<sup>‡</sup>Electronic address: thomas.witkowski@tu-dresden.de

is rotationally invariant arbitrary orientations of periodic structures can emerge. Furthermore the model allows the formation of dislocations, which occur when two periodic structures of different orientation collide or when it is energetically favorable for them to nucleate. The PFC model has been used to simulate various crystal growth phenomena including epitaxial growth, nucleation, commensurate-incommensurate transitions and plastic deformations. In [17] is shown how the model can be derived from a microscopic Smoluchowski equation via dynamical density functional theory. Formulating the energy in Eq. (1) on a curved surface  $\Gamma$  leads to

$$\mathcal{F}^\Gamma[\rho] = \int_\Gamma -|\nabla_\Gamma \rho|^2 + \frac{1}{2}|\Delta_\Gamma \rho|^2 + f(\rho) d\Gamma \quad (2)$$

with  $\rho$  as the number density on  $\Gamma$ , as well as  $\nabla_\Gamma$  and  $\Delta_\Gamma$  as the surface gradient and surface Laplacian, respectively. We will use the  $H^{-1}$  gradient flow of this energy to solve the generalized Thomson problem and to analyze the dynamics of rearrangements of particles on a curved surface. The equation, written as a system of three second order equations, reads as

$$\partial_t \rho = \Delta_\Gamma u \quad (3)$$

$$u = \Delta_\Gamma v + 2v + f'(\rho) \quad (4)$$

$$v = \Delta_\Gamma \rho. \quad (5)$$

The stable finite element discretization for the PFC model in the plane introduced in [18] can be adapted to solve Eqs. (3)-(5) on a surface triangulation using parametric finite elements. The key idea is to use the surface operators on the discrete surface which consists of triangles  $T$ . To do the integration on these triangles a parametrization  $F_T : \hat{T} \rightarrow T$  is used, with  $\hat{T}$  as the standard element in  $\mathbb{R}^2$ . These allow us to transform all integrations onto the standard element using the finite element basis defined also only in  $\mathbb{R}^2$ . The parametrization  $F_T$  is given by the coordinates of the surface mesh elements and provides the only difference between solving equations on surfaces and on planar domains. For a surface we have to allow  $F_T : \mathbb{R}^2 \rightarrow \mathbb{R}^3$ , whereas for a planar domain  $F_T : \mathbb{R}^2 \rightarrow \mathbb{R}^2$ . With this tiny modification any code to solve partial differential equations on Cartesian grids can be used to solve the same problem on a surface, providing a surface triangulation is given. The computational cost is the same as solving the problem in a planar domain. Within an efficient implementation this does not even require to recompile a running two-dimensional (2D) code, but only a change in a parameter file, as e.g. done in AMDiS [19]. With this approach all available tools to solve partial differential equations on planar domains, such as adaptive refinement, multigrid algorithms or parallelization approaches are available also to solve equations on surfaces.

The approach is used to evolve a randomly perturbed constant initial configuration  $\rho = \rho_0$  towards an energy minimum. With the possibilities to use adaptive time stepping and the efficiency of parallelization of the finite

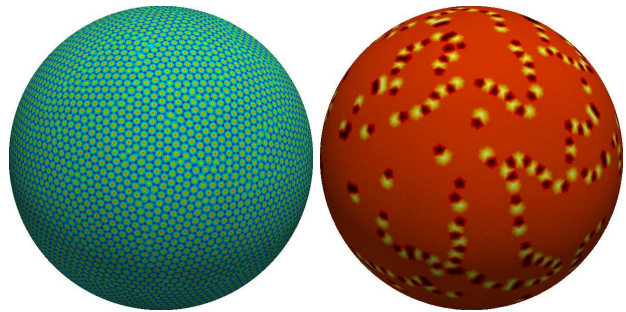


FIG. 1: (Color online) Local minimal energy configuration for 6.064 particles on a sphere. (left) density profile, (right) color coded number of neighbors, 5-black, 6-red (gray) and 7-yellow (white).

element method problem sizes of  $1 \times 10^6$  particles can be addressed. The simulation for Fig. 1 with 6.064 particles required 1 day computing time on a single processor.

In order to validate our approach we compute minimal energy configurations for various numbers of  $N$ . We systematically compute the minimal energy configuration for all  $N \in [12, 2790]$ . In our configuration  $N = 2790$  corresponds to  $r = 100$ . The numerical results indicate, that the obtained minimal energy configurations are only sensitive to the defined lattice spacing and insensitive to a large extent to the other parameters. This might explain why triangular tessellations on spherical surfaces occur in very distinct occasions, for which the interactions involved may differ a lot. In the following we use  $\rho_0 = -0.3$  and  $\epsilon = 0.4$ , which together with the radius  $r$  of the sphere determines  $N$ . For all  $N$  the type and number of disclinations, as well as the computed energy is in agreement with known analytical or other numerical results. For  $N \leq 112$  the configurations and energies coincide with the known equilibrium values. The maximal deviation from the minimal energy for larger  $N$  is less than 0.1 %. Table I shows computed configurations for

TABLE I: Comparison with known results for small  $N$ . In order to compute the energy we identify the position of the maxima in the density field and compute the Coulomb energy according to this positions.

<b>N</b>	<b>v4</b>	<b>v5</b>	<b>v6</b>	<b>v7</b>	<b>v8</b>	<b>energy</b>
63	0	12	51	0	0	1708.87968150
99	0	12	87	0	0	4357.13916313
130	0	13	116	1	0	7632.16737891
185	0	12	173	0	0	15723.72346397
222	0	13	208	1	0	22816.07553076
363	0	14	347	2	0	62066.53633167
684	0	33	630	21	0	224048.60512144
846	0	38	782	26	0	344267.84965308
1073	0	45	995	33	0	556250.19927822
1403	0	54	1307	42	0	955173.65896550
2726	0	78	2584	64	0	3636897.41372145

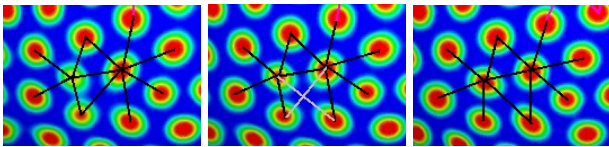


FIG. 2: (Color online) Annihilation of dislocation by local rearrangement of 5-7 defect. The gray lines indicate the formation of a new neighbour at an intermediate state.

selected  $N$ . For  $N > 360$  we obtain additional defects in the ground state, which are pairs of fivefold and sevenfold coordinated particles (dislocations) and chains of alternation fivefold and sevenfold coordinated particles (grain-boundary scars). Since dislocations have vanishing total disclination charge there can be an arbitrary number of them in any spherical lattice configuration without violating the topological constraint on the total disclination charge discussed above. The grain-boundary scars found are unlike any grain boundaries found in flat space as they terminate freely inside the crystal at both ends. Due to the importance of dislocations and grain boundaries in bulk materials in determining material properties similar roles can be expected on surfaces. In [13] the motion of dislocations is observed experimentally. Dislocation motion can be separated into glide and climb, where glide is motion parallel to the dislocation's Burger vector and requires only local rearrangement of the lattice, and climb is motion perpendicular to the Burger's vector and requires the presence of vacancies and interstitials. In agreement with the observations in [13] and the computational results based on elasticity in [12] we also observe only glide motion which leads to significant shape changes of the scars. Fig. 2 shows a local rearrangement of a dislocation.

In [14] the question is asked which effect a raising of temperature has on the spherical crystal. For bulk polycrystalline material there is indirect experimental evidence for the occurrence of grain boundary premelting, which could directly be visualized for colloidal crystals in [20]. As a liquid film at grain boundaries will alter macroscopic properties and especially will lead to a drastically reduced resistance to shear stresses which can lead to material failure it is not only of theoretical interest if grain-boundary premelting is also present in spherical crystals. As grain-boundary scars belong to the equilibrium state it would be even more severe as it would be a general property of crystalline materials on curved surfaces. PFC models have already been used to study grain-boundary premelting in flat space [21, 22]. For high-angle grain boundaries a uniformly wetting is observed below the melting temperature in these studies. Raising the temperature (increasing  $\epsilon$ ) but keeping it below the melting temperature according to the phase diagram indeed leads to melting of the grain-boundary scars, see Fig. 3.

We use the premelting of the dislocations to improve the local minima our evolution settles in. Within an it-

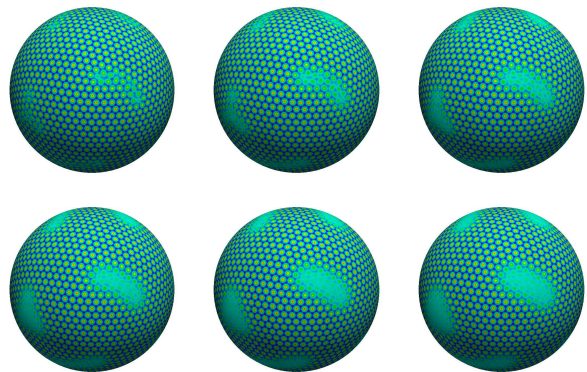


FIG. 3: (Color online) Time sequence showing premelting at grain boundary scars. The simulations indicate an initiation of the melting at the ends of the scars.

erative procedure we evolve the system according to Eqs. (3) - (5) until we reach a minimal state, increase the temperature and run the system until liquid layers have replaced all dislocations, and start the evolution again with the original temperature. The algorithm is terminated if the total energy does not further decrease. Typically this is achieved after 2-3 iteration cycles. In Figure 4 we plot the excess dislocations in a scar as a function of the system size  $\sqrt{N} = r/a$ .

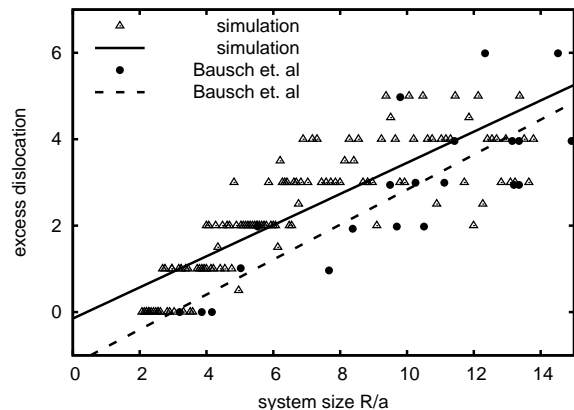


FIG. 4: Excess dislocations as a function of system size. The obtained slope is  $0.388 \pm 0.020$ , which is in excellent agreement with the experimental measured data in [4], which give  $0.404 \pm 0.062$ , and the theoretical value of 0.41 from [10]

As already pointed out the method is not restricted to spherical geometries. Indeed the algorithm works for arbitrary surfaces with the only requirement that an appropriate surface mesh is needed on which the computation can be done. As an example we use toroidal crystals, which can be found e.g. in self-assembled monolayers of micelles and vesicles [24] or carbon nanotori [25]. We compute low energy configurations for various toroidal

lattice configurations and reach good comparison with results reported in [26]. Fig. 5 shows a typical configuration for aspect ratio  $R_1/R_2 = 2.78$ .

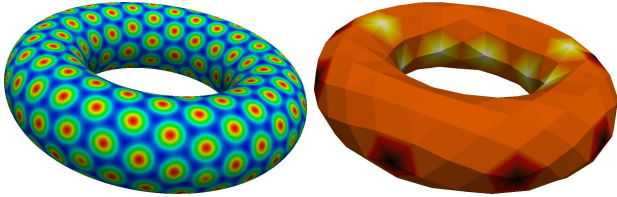


FIG. 5: (Color online) Minimal energy configuration on torus with  $N = 239$ , there are 13 fivefold disclinations and 13 sevenfold disclinations, 5-black, 6-red (gray) and 7-yellow (white).

In computations on more complicated surfaces, with convex and concave regions, we observe isolated fivefold and sevenfold disclinations which arrange according to the local curvature of the surface. Thereby fivefold disclinations are preferably found in convex regions, whereas sevenfold disclinations are present in concave regions, which is in accordance with the theory discussed in [23]. The ability of the approach to work on arbitrary surfaces will also allow us to consider ordering on evolving surfaces. As discussed above for low surface tensions a buck-

ling transition of the disclinations can turn the sphere into a polygon in order to reduce the energy. The question arises if such a transition can intervene with grain boundary scar formation. In [27] it is speculated that grain boundary scars could be formed on capsids at an intermediate stage of their evolution and that the release of the bending energy present in these scars into stretching energy could allow for shape changes. To model such shape changes requires us to evolve the surface. Appropriate continuum models which account for bending and surface tension are discussed in the mathematical review papers [28, 29]. Different concepts have been developed to solve differential equations on evolving surfaces, [30] in the context of parametric finite elements (as considered here) and [31] within a phase-field context. The coupling of the surface evolution with the evolution of the number density on it and with it the question if grain boundary scars can initiate a buckling transition, however remains open and requires further developments.

### Acknowledgments

This work was supported by German Science Foundation Grants No. VO899/6-1 and No. VO899/6-2.

- 
- [1] J.J. Thomson, *Philos. Mag.* **7**, 237 (1904).
  - [2] J. Lidmar, L. Mirny, and D.R. Nelson, *Phys. Rev. E* **68**, 051910 (2003).
  - [3] R. Zandi, D. Reguera, R.F. Bruinsma, W.M. Gelbart, and J. Rudnick, *Proc. Nat. Acad. Sci.* **101**, 15556 (2004).
  - [4] A.R. Bausch, M.J. Bowick, A. Cacciuto, A.D. Dinsmore, M.F. Hsu, D.R. Nelson, M.G. Nikolaides, A. Travesset, and D.A. Weitz, *Science* **299**, 1716 (2003).
  - [5] L. Ramos, T.C. Lubensky, N. Dan, P. Nelson, and D.A. Weitz, *Science* **286**, 2325 (1999).
  - [6] A.D. Dinsmore, M.F. Hsu, M.G. Nikolaides, M. Marquez, A.R. Bausch, and D.A. Weitz, *Science* **298**, 1006 (2002).
  - [7] K. Stratford, R. Adhikari, I. Pagonabarraga, J.C. Desplat, and M.E. Cates, *Science*, **309**, 2198 (2005).
  - [8] Y.G. Sun, W.M. Choi, H.Q. Jiang, Y.Y. Huang, and J.A. Rogers, *Nat. Nanotechnol.* **1**, 201 (2006).
  - [9] T. Erber, and G.M. Hockney, *J. Phys. A* **24**, L1369 (1991).
  - [10] M.J. Bowick, D.R. Nelson, and A. Travesset, *Phys. Rev. B* **62**, 8738 (2000).
  - [11] M.J. Bowick, A. Cacciuto, D.R. Nelson, and A. Travesset, *Phys. Rev. Lett.*, **89**, 185502 (2002).
  - [12] M. Bowick, H. Shin, and A. Travesset, *Phys. Rev. E* **75**, 021404 (2007).
  - [13] P. Lipowsky, M.J. Bowick, J.H. Meinke, D.R. Nelson, and A.R. Bausch, *Nature Materials*, **4**, 407 (2005).
  - [14] X.S.S. Ling, *Nature Materials*, **4**, 360 (2005).
  - [15] J. Swift, and P.C. Hohenberg, *Phys. Rev. A*, **15**, 319 (1977).
  - [16] K.R. Elder, M. Katakowski, M. Haataja, and M. Grant, *Phys. Rev. Lett.*, **88**, 245701 (2002).
  - [17] S. van Teeffelen, R. Backofen, A. Voigt, and H. Löwen, *Phys. Rev. E*, **79**, 051404 (2009).
  - [18] R. Backofen, A. Rätz, and A. Voigt, *Phil. Mag. Lett.*, **87**, 813 (2007).
  - [19] S. Vey, and A. Voigt, *Comput. Vis. Sci.*, **10**, 57 (2007).
  - [20] A.M. Alsayed, M.F. Islam, J. Zhang, P.J. Collings, and A.G. Yodh (2005) Premelting at defects within bulk colloidal crystals *Science* 309:1207-1210.
  - [21] J. Berry, K.R. Elder, and M. Grant, *Phys. Rev. B*, **77**, 224114 (2008)
  - [22] J. Mellenthin, A. Karma, and M. Plapp, *Phys. Rev. B*, **78**, 184110 (2008).
  - [23] V. Vitelli, J.B. Lukas, and D.R. Nelson, *Proc. Nat. Acad. Sci.*, **103** 12323 (2006).
  - [24] J.K. Kim, E. Lee, Z.G. Huang, and M. Lee, *J. Ame. Chem. Soc.*, **128** 14022 (2006).
  - [25] J. Liu, H. Dai, J.H. Hafner, D.T. Colbert, R.E. Smalley, S.J. Tans, and C. Dekker, *Nature*, **385** 780 (1997).
  - [26] L. Giomi, and M.J. Bower, *Phys. Rev. E*, **78** 010601 (2008).
  - [27] A. Iorio, and S. Sen, *Cen. Eur. J. Biol.*, **3** 380 (2008).
  - [28] K. Deckelnich, G. Dziuk, and C.M. Elliott, *Acta Num.*, **14** 139 (2005).
  - [29] B. Li, J. Lowengrub, A. Rätz, and A. Voigt, *Comm. Comp. Phys.*, **6** 433 (2009).
  - [30] G. Dziuk, and C.M. Elliott, *IMA J. Num. Ana.*, **27** 262 (2007).
  - [31] A. Rätz, and A. Voigt, *Nonlin.*, **20** 177 (2007).